Dynamic Magnetic Response Across the Pressure-Induced Structural Phase Transition in CeNi

A. Mirmelstein

Department of Experimental Physics
Russian Federal Nuclear Center – E.I. Zababakhin Institute of Technical Physics (RFNC-VNIITF)
Snezhinsk, Chelyabinsk region, Russia

Outline

- **Motivation**
- **Why CeNi?**
- **Structural behavior of CeNi under pressure**
- **Magnetic dynamics of CeNi before and after structural transition**
- **Conclusions**

Dynamic Magnetic Response Across the Pressure-Induced Structural Phase Transition in CeNi

In collaboration with

RFNC-VNIITF

V. Matvienko
O. Kerbel

Sample

B. Saparov — Materials Science and
A.S. Sefat — Engineering Div., **ORNL**

Neutron scattering

A. Podlesnyak — Quantum Condensed
G. Ehlers — Matter Science Div. **ORNL**
D.L. Abernathy — ORNL
Antonio M. dos Santos

A.I. Kolesnikov — Chemical and Engineering Materials Div., **ORNL**

X-ray diffraction

G.J. Halder — X-Ray Science Division, **ANL**

Special thanks are addressed to Andrey Podelsnyak, Sasha Kolesnikov (ORNL) and James G. Tobin (LLNL) for their long-term support and contribution to this study.

Motivation

The main problem of interest:

mechanisms underlining the pressure-induced first-order structural phase transition with volume jump in f-electron systems

The problem is closely related to understanding crossover between the local moment and itinerant f electron behavior.

The most famous examples are:

- the isostructural volume-collapse $\gamma \rightarrow \alpha$ transition in Ce metal
- $\delta \rightarrow \alpha$ transformation in plutonium metal ($\delta \rightarrow \alpha'$ in fcc Pu-Ga alloy)

Dynamic Magnetic Response Across the Pressure-Induced Structural Phase Transition in CeNi

Isostructural volume-collapse $\gamma \rightarrow \alpha$ transition in Ce metal

$\Delta V/V$ ~ 15-17%

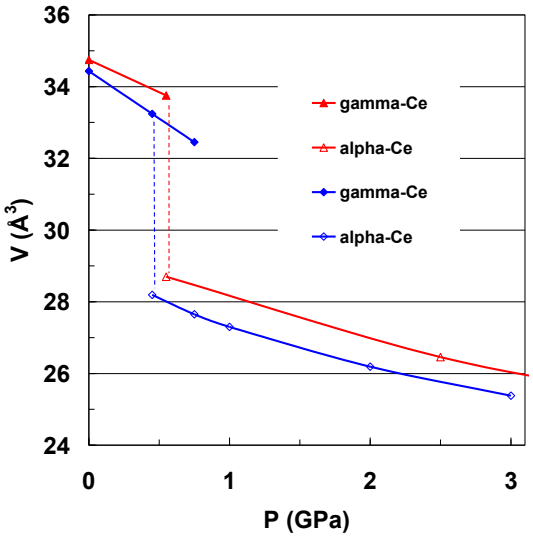

Atomic volume $V = a^3/4$ of Ce vs. pressure at room temperature. *a* is the crystal lattice parameters. Blue signs - data by W.H. Zachariazen and F.H. Ellinger, Acta Cryst. A33 (1977) 155. Red signs – VNIITF data.

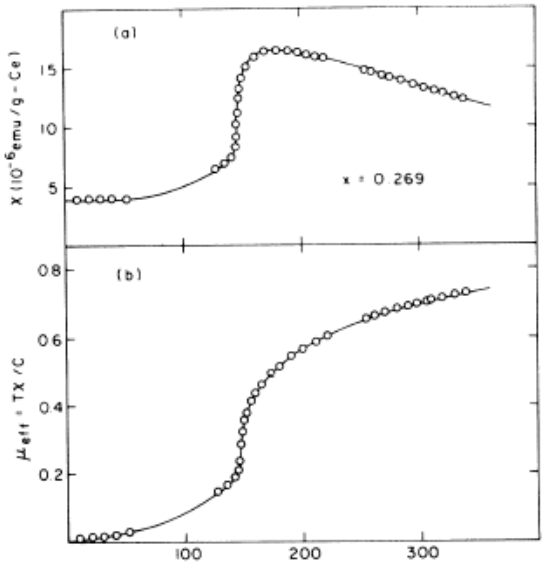

(a) dc bulk magnetic susceptibility χ(T) for $Ce_{0.721}Th_{0.269}$.
(b) The effective moment $\mu_{eff} = T\chi/C$ should saturate to unity at high T.
S.M. Shapiro et al., PRB 16 (1977) 2225.

Replacement of the normal Curie-Weiss T-dependence in χ(T) of γ phase (indicative of a local moment behavior) by a practically T-independent susceptibility in α-Ce (suggesting a quenched moment state).

Dynamic Magnetic Response Across the Pressure-Induced Structural Phase Transition in CeNi

$\delta \rightarrow \alpha'$ transformation in fcc Pu-Ga alloy

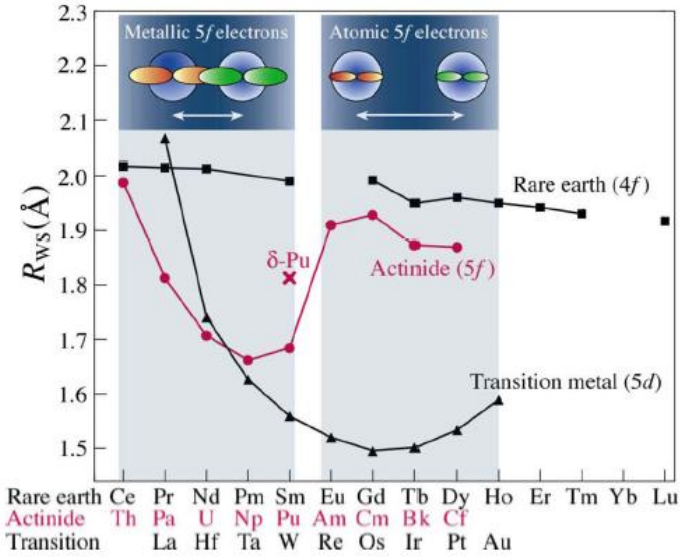

Wigner-Seitz radius of each metal as a function of atomic number Z for the 5d, 4f, and 5f metal series. From A.M. Boring and J.L. Smith, in *Challenge in Plutonium Science*, 2000, Vol. I (Los Alamos Science, Los Alamos, NM) No. 26. p.91.

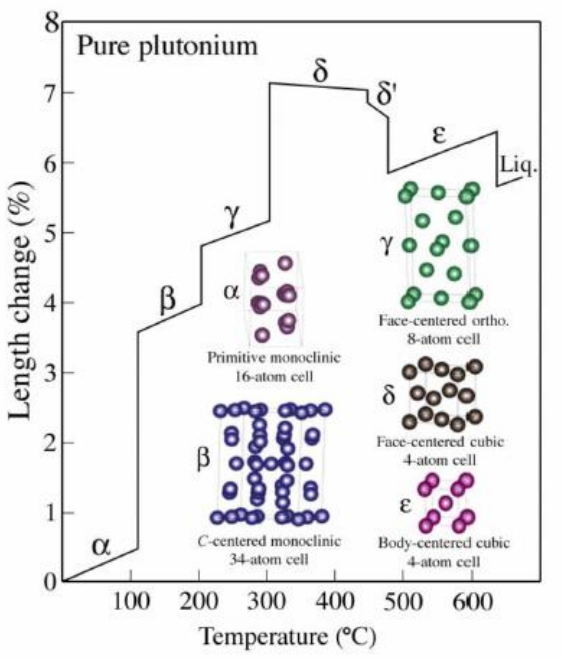

Relative length change as a function of temperature for the pure Pu metal [S. Hecker, ibid, Vol. II, No. 26 p. 290].

Volume difference between α- and δ- phases is ~ 25%

Dynamic Magnetic Response Across the Pressure-Induced Structural Phase Transition in CeNi

δ→α‘ transformation in fcc Pu-Ga alloy

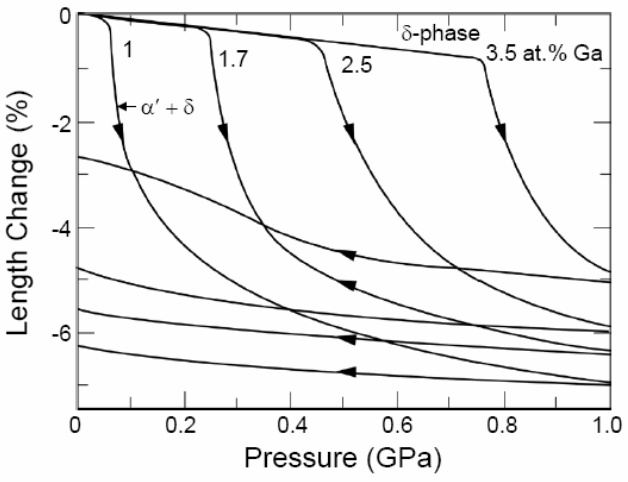

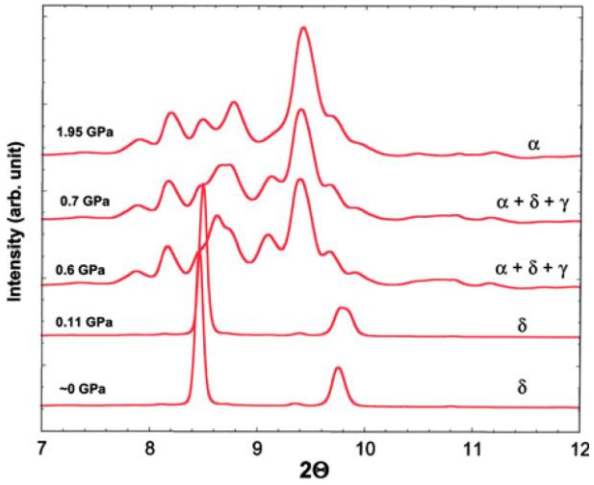

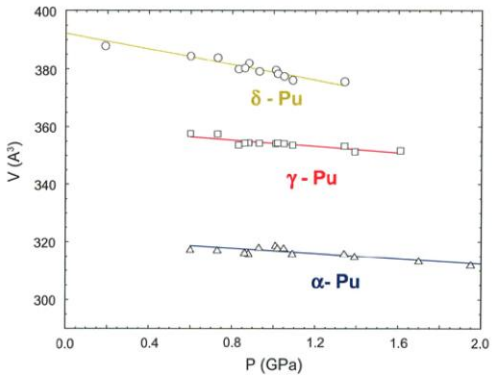

Pressure-induced δ→ α′ transformation in fcc Pu-Ga alloys [S. Hecker, 2011].

δ phase directly transforms to α′

X-ray diffraction pattern of pressure-induced δ→ α′ transition in Pu-3.3%at.Ga [A. Schwartz et al., Progress in Materials Science, 2009]

Both α′- and γ′- phases arise simultaneously under pressure

Many features of this transition still have no explanation, including stabilization of the fcc phase by alloying different elements, influence of defects and strains on the transformation etc.

Dynamic Magnetic Response Across the Pressure-Induced Structural Phase Transition in CeNi

Why CeNi?

- ***CeNi is an intermediate-valence system experiencing pressure-induced structural instability*** **[D. Gignoux, F. Givord, and R. Lemaire, J. Less-Common Metals 94 (1983) 165].**

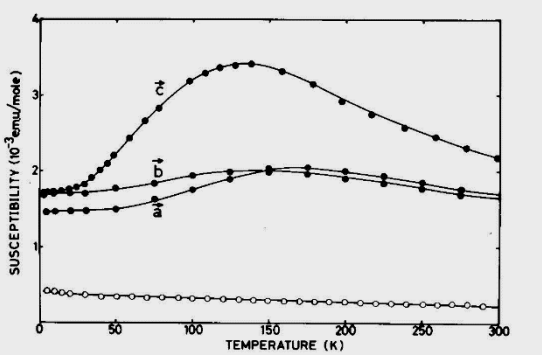

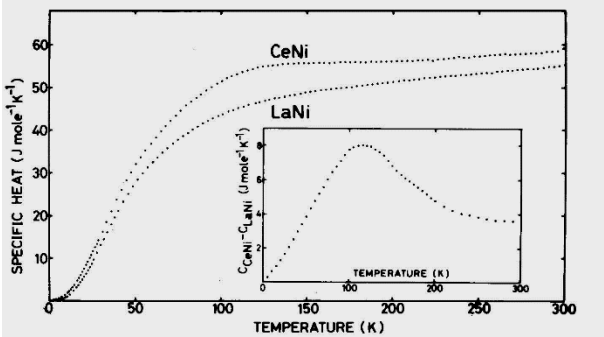

Specific heat vs. *T* for CeNi and LaNi. Inset: $\Delta C = C_{CeNi} - C_{LaNi}$.

Magnetic susceptibility vs. temperature for CeNi (•) in a field of 50 kOe applied along the *a*, *b*, and *c* axes of the orthorhombic structure and the susceptibility of polycrystalline LaNi (o)

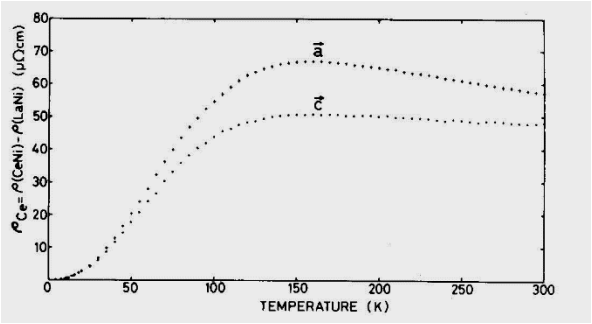

Thermal variation of resistivity $\rho_{Ce} = \rho_{CeNi} - \rho_{LaNi}$ along the *a* and *c* axes.

Why CeNi?

CeNi has the CrB-type orthorhombic crystal structure (space group Cmcm) repeatedly appearing in rare-earth and actinide metals under pressure, e.g., α'-Ce, Pa, Nd, Pr, Am IV, and α-U.

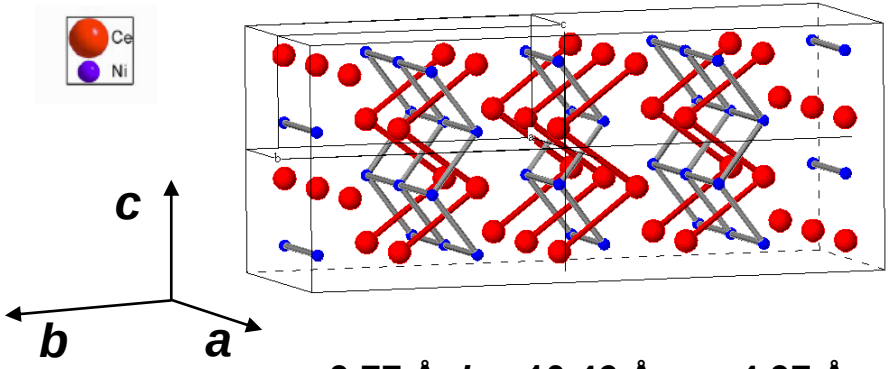

***a* = 3.77 Å, *b* = 10.46 Å, *c* = 4.37 Å**
Ce: 4c (0, 0.139, 1/4)
Ni: 4c (0, 0.428, 1/4)

J. Tinney and A. Rosenzwieg, Acta Cryst. 14, 69 (1961)

Dynamic Magnetic Response Across the Pressure-Induced Structural Phase Transition in CeNi

Why CeNi?

- *CeNi experiences pressure-induced first-order structural phase transition.*

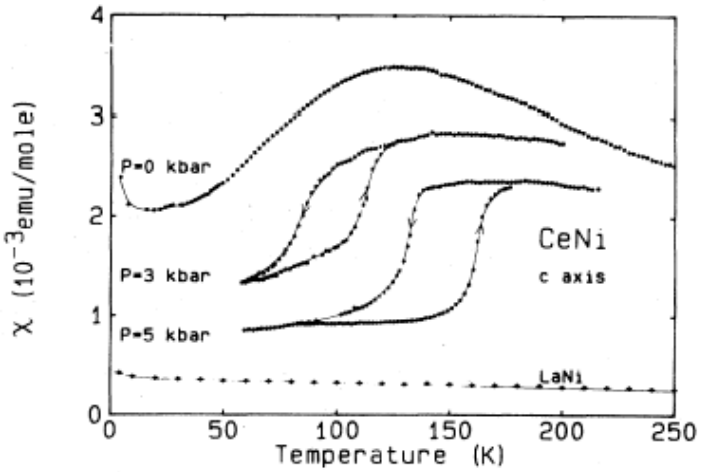

FIG. 1. Thermal variations of the susceptibility of CeNi measured along the c axis of the orthorhombic cell at room pressure and under 3 and 5 kbar. Thermal variation of the susceptibility of a polycrystalline sample of LaNi at room pressure.

D. Gignoux and J. Voiron
PRB 32, 4822 (1985)

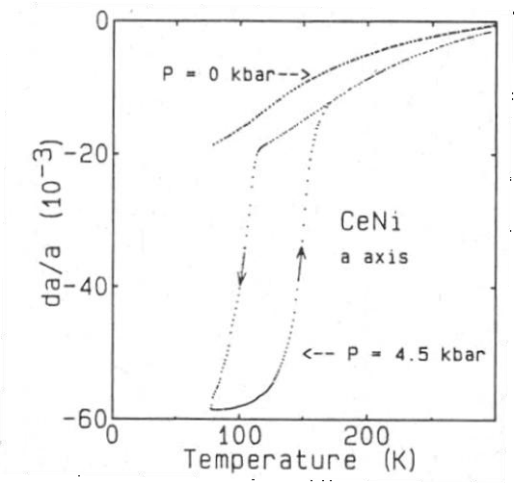

~ 5% volume change under transition

D. Gignoux, C. Vettier and J. Voiron JMMM 70, 388 (1987)

The structure of CeNi high pressure phase remained unknown for a long time (since 1985). Study of the structural transition in this compound can be useful to better understand the behavior of similar structures under pressure.

Dynamic Magnetic Response Across the Pressure-Induced Structural Phase Transition in CeNi

Why CeNi?

• *As soon as the Ce valence in intermediate-valence CeNi differs significantly form integer value, one can expect the volume-collapse structural phase transition to shift the system towards the itinerant (bonding) f electron behavior (in this sense structural transition in CeNi can be considered as an analog of $\delta \rightarrow \alpha'$ transformation in plutonium)*

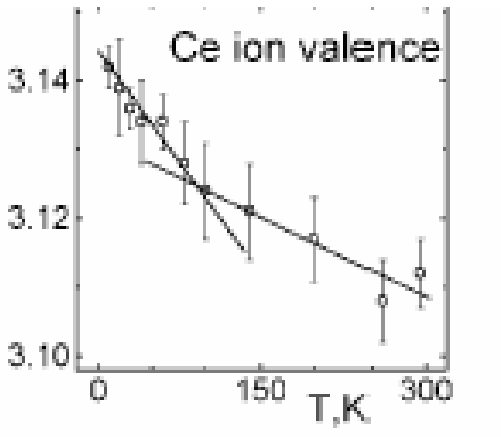

Temperature dependence of Ce valence in CeNi

V.N. Lazukov et al.,
Appl. Phys. A74 [Suppl.], S559 (2002)

The aim of this work is to determine the crystal structure of the CeNi high pressure phase using x-ray and neutron powder diffraction and to study the variation of magnetic excitation spectrum in CeNi due to structural transition by means of INS technique

Dynamic Magnetic Response Across the Pressure-Induced Structural Phase Transition in CeNi

Experimental

Structural investigations:

powdered CeNi sample (natural mixture of Ni isotopes)

high-pressure synchrotron x-ray measurements, beamline 17-BM-B, APS (ANL)

T=298 K, pressure up to 7.8 GPa

neutron powder diffrcation, SNS (ORNL) SNAP diffractometer

T=100 K, pressure up to 5.05 GPa

details: A. Mirmelstein et al., PRB 92, 054102 (2015)

Inelastic neutron scattering SNS, ORNL:

polycrystalline CeNi sample of ~3 g in mass, ^{60}Ni isotope (enrichment ~99%)

^{60}Ni nuclear cross section σ_S = 1.0 b
natural isotope mixture compared to σ_S = 18.5 b
magnetic cross section of Ce^{3+} ions $\sigma_M \approx$ 3.7 b

INS spectra of CeNi were measured using fine-resolution Fermi chopper spectrometer SEQUOIA, T=20 K, ambient pressure, P = 0.4 GPa

Magnetic formfactor was measured with ARCS (wide angular-range chopper spectrometer) instrument
T=20 K, ambient pressure, P = 0.45 GPa

Pressure was generated using the Al pressure cell with He gas as a pressure transmitting medium

Dynamic Magnetic Response Across the Pressure-Induced Structural Phase Transition in CeNi

Structure of CeNi high pressure-phase

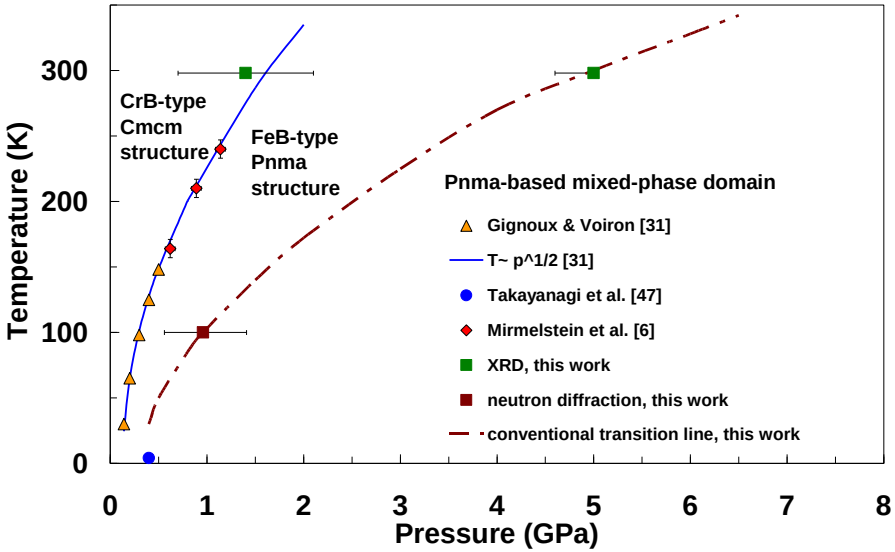

***P-T* phase diagram of CeNi as follows from the present diffraction (green and brown squares), magnetic (yellow triangles and red circles), and specific heat measurements. Blue solid line – empirical transition line suggested by Gignoux and Voiron (1985).**

<u>At room temperature</u>:

First structural transformation occurs around *P* ~ 1 GPa.

CrB (C*mcm* space group) structure transforms to the FeB-type of structure (P*nma* space group). $\Delta V/V=1.3\%$ at P = 1.17 GPa

Second transformation occurs around 5 GPa

FeB $\rightarrow$ P*nma*-based mixed phase state FeB+3×a_{FeB}

(explanation below)

Dynamic Magnetic Response Across the Pressure-Induced Structural Phase Transition in CeNi

CeNi Low Pressure (LP) phase

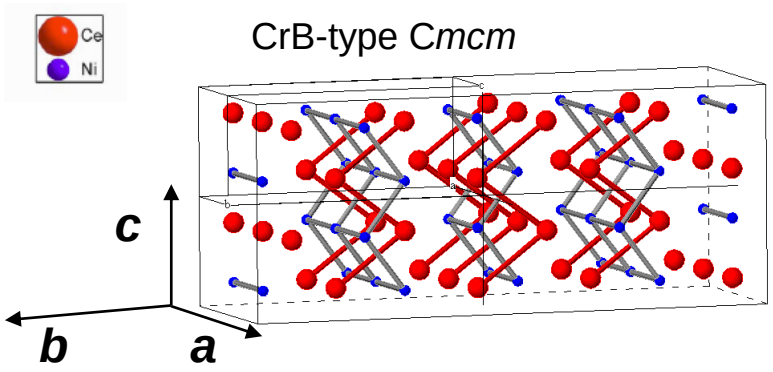

P=0.7 GPa (below transition)

***a* = 3.771(2) Å, *b* = 10.529(8) Å, *c* = 4.366(2) Å**
Ce: 4c 0, 0.14(1), 1/4
Ni: 4c 0, 0.42(1), 1/4

A. Mirmelstein, PRB (2015)

CeNi High Pressure (HP) phase

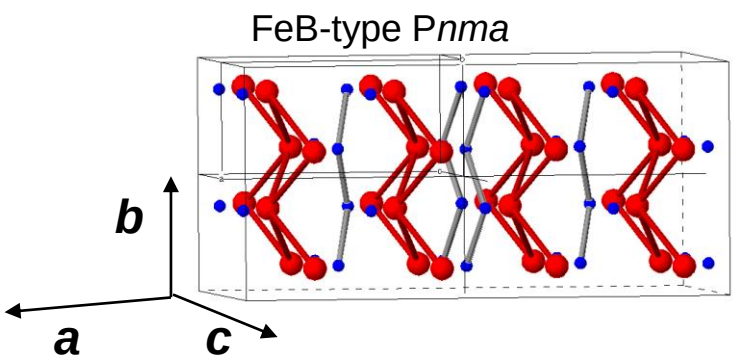

P=4.2GPa

***a* = 7.161(5) Å, *b* = 4.390(4) Å, *c* = 5.086(4) Å**
Ce: 4c 0.13(1), 1/4, 0.20(1)
Ni: 4c 0.09(1), 1/4, 0.66(1)

The FeB structure is typical for the RNi compounds where R is the rare-earth metal from the second half of the lanthanide series, while light lanthanides, including cerium, form the crystal lattice of the CrB type [A.E. Dwight, R.A. Conner, Jr., J.W. Downey, Acta Cryst. **18**, 837 (1965)]

Both the FeB and CrB structural types contain a common structural unit, the trigonal prism, which is stacked differently to form either structure [R. Lemaire and D. Paccard, Journal of the Less-Common Metals **21**, 403(1970)].

Dynamic Magnetic Response Across the Pressure-Induced Structural Phase Transition in CeNi

If the z value of the 4c sites in the Pnma structure goes to zero, one obtains the higher-symmetry Cmcm structure

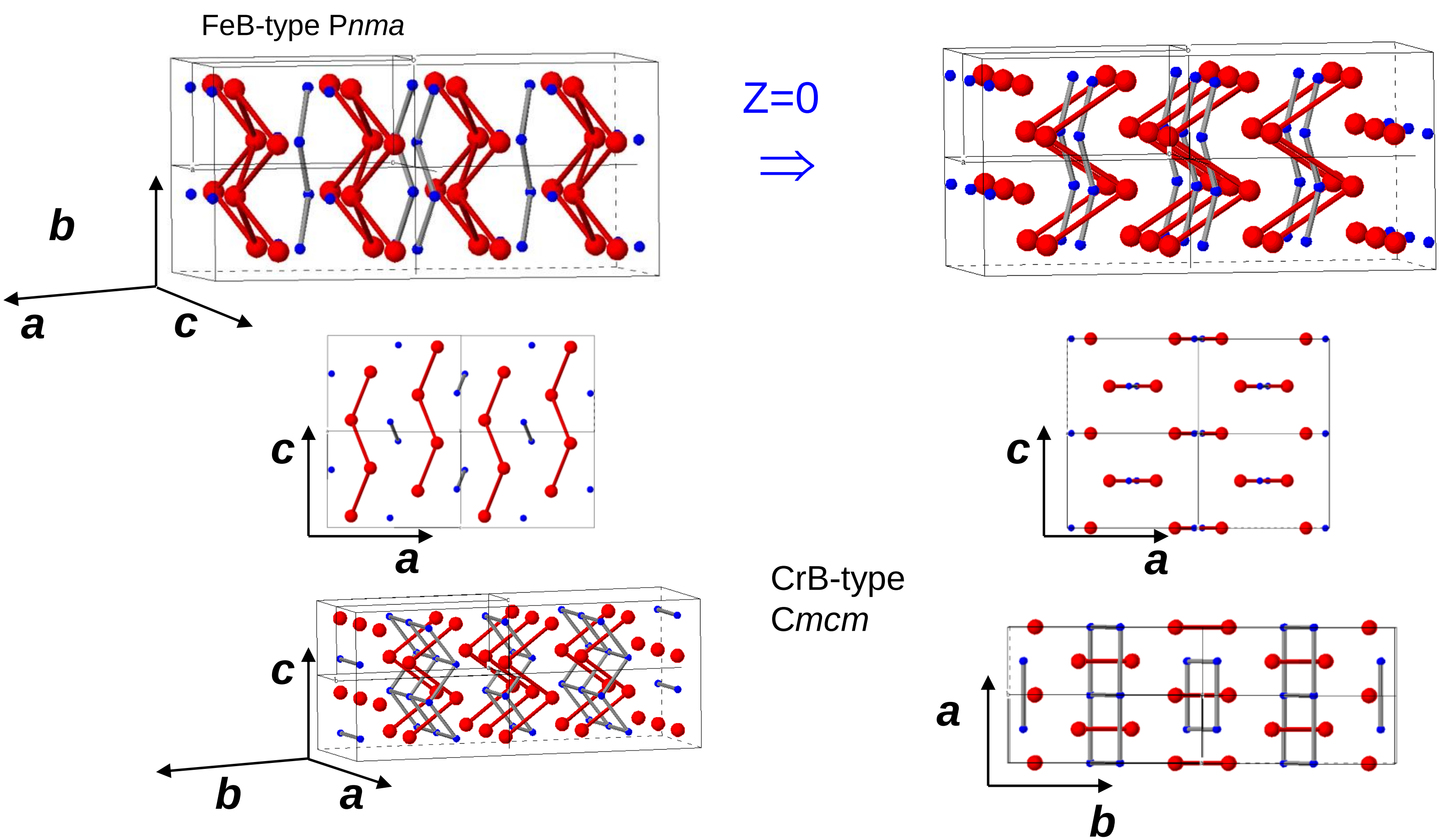

Dynamic Magnetic Response Across the Pressure-Induced Structural Phase Transition in CeNi

Structure of CeNi high pressure-phase

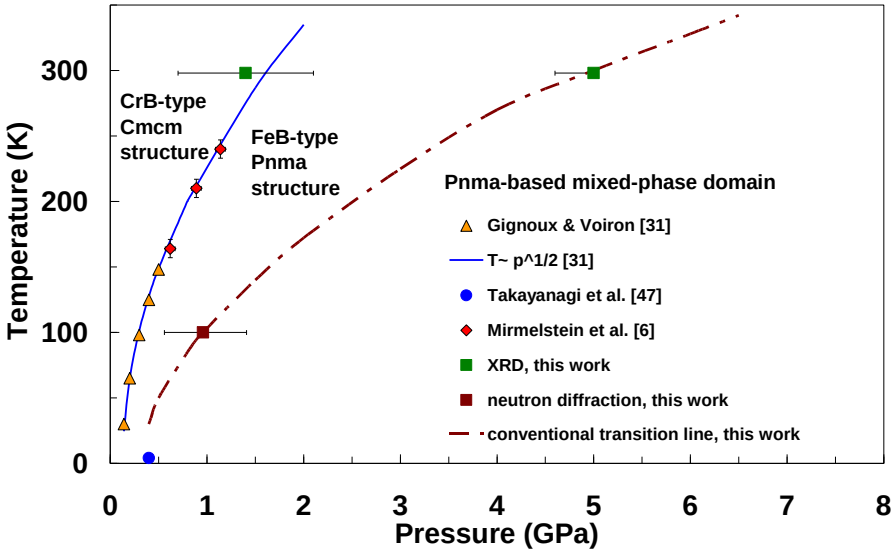

***P-T* phase diagram of CeNi as follows from the present diffraction (green and brown squares), magnetic (yellow triangles and red circles), and specific heat measurements. Blue solid line – empirical transition line suggested by Gignoux and Voiron (1985).**

At T = 100 K:

Pure FeB Pnma structure was not found. At P above 1 GPa the neutron powder diffraction patterns are described by a new orthorhombic cell with crystal lattice parameters $a=3\times a_{FeB}$; $b=b_{FeB}$; $c=c_{FeB}$

$3\times a_{FeB}Pnma$

This structure is similar to the structure of quenched modification of the TbNi compound [R. Lemaire and D. Paccard, Journal of the Less-Common Metals **21**, 403(1970)]

$\Delta V/V$=7.9% at P = 0.96 GPa

Dynamic Magnetic Response Across the Pressure-Induced Structural Phase Transition in CeNi

Structure of CeNi high pressure-phase

R. Lemaire and D. Paccard, Journal of the Less-Common Metals **21**, 403(1970)

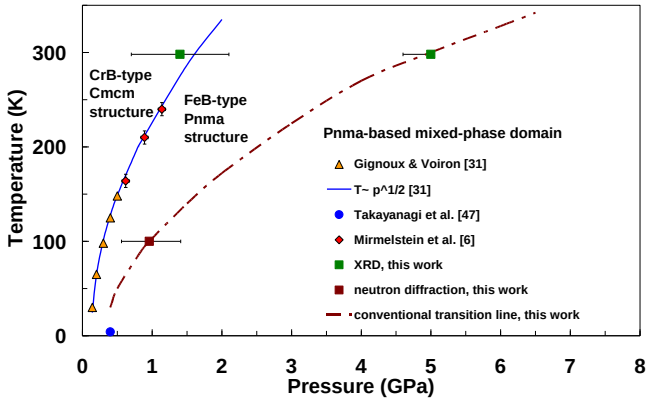

***P-T* phase diagram of CeNi**

$$a_{TbNi} = 3a_{FeB}$$
$$b_{TbNi} = c_{FeB},.$$
$$c_{TbNi} = c_{FeB}$$

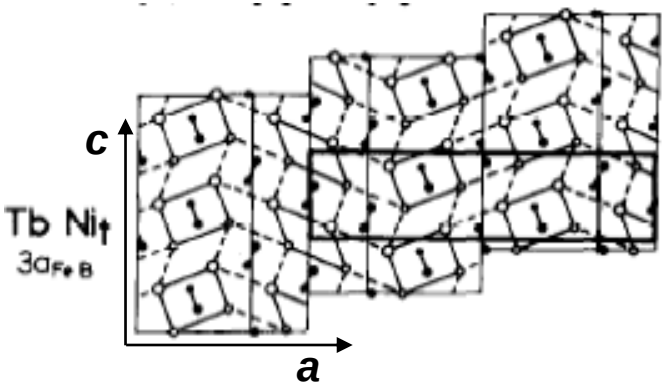

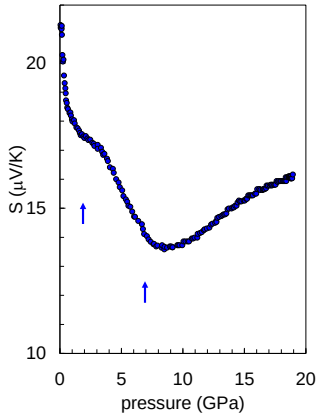

Thermopower vs. pressure for CeNi at *T*=300 K

A. Mirmelstein et al.

(2007)

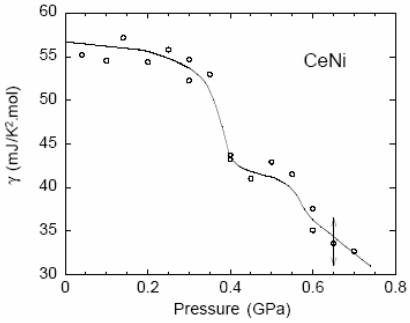

Specific heat coefficient γ vs. pressure for CeNi

S. Takaynagi et al., J. Phys. Soc. Jap. 70 (2001) 753

These previous experiments seem to confirm two transitions for both low and room temperature

Dynamic Magnetic Response Across the Pressure-Induced Structural Phase Transition in CeNi

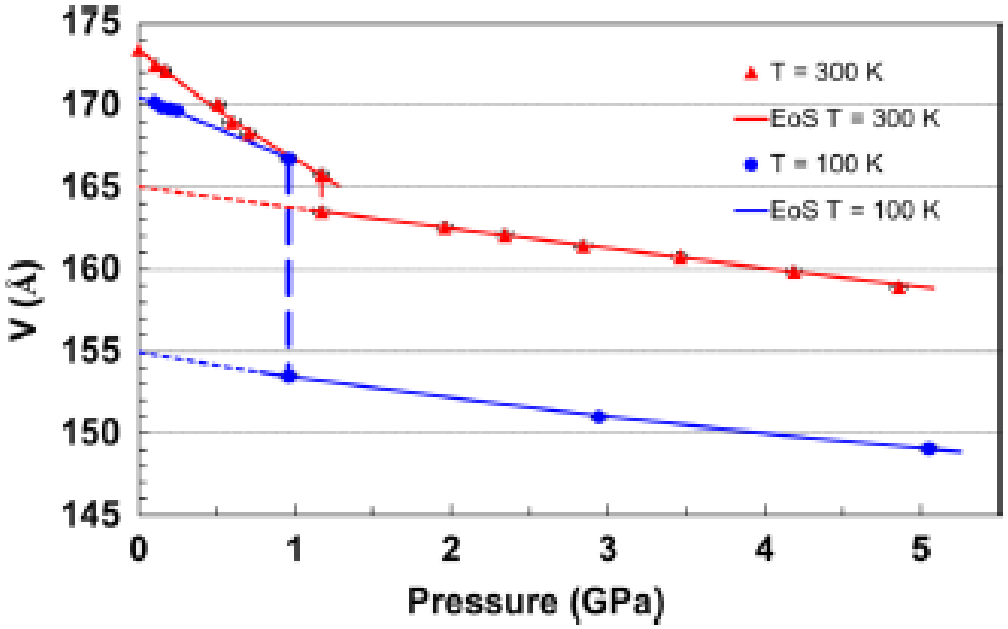

Equation o State for CeNi at T = 300 K and T = 100 K.

Solid lines are the results of fitting the measured unit cell volume to a third-order Birch-Murnaghan EOS [F. Murnaghan, PNAS 30, 244 (1944), F. Birch, Phys. Rev. 71, 809 (1947)].

Фазовые переходы с коллапсом объема в f-электронных системах: CeNi

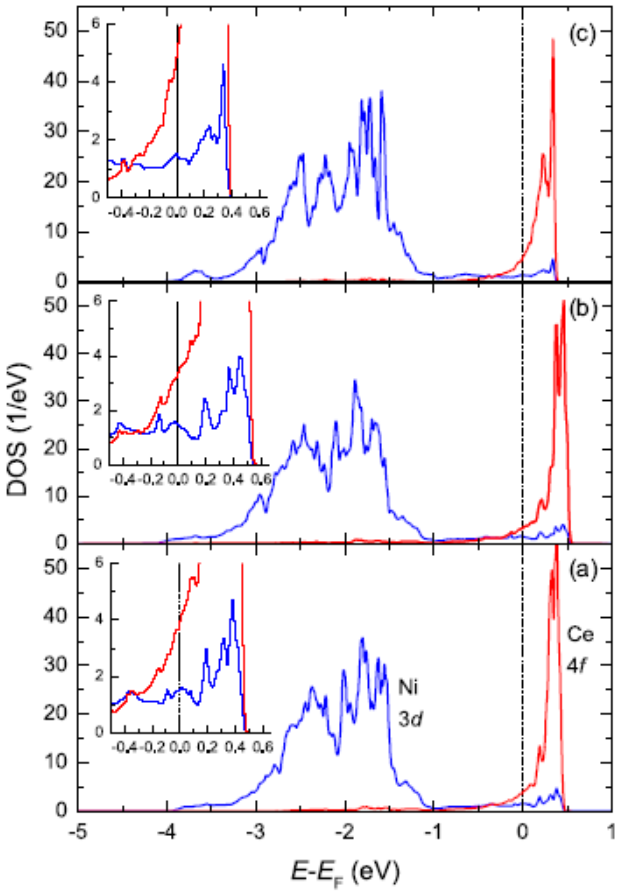

Парциальные плотности состояний для (a) CeNi C*mcm* фазы при нормальном давлении, (b) *Cmcm* фазы при *P* = 1 ГПа и (c) P*nma* фазы при *P* = 1 ГПа.

На вставках – те же DOS вблизи E_F в увеличенном масштабе.

Signature of increased f-d hybridization can be seen in panel (c).

Dynamic Magnetic Response Across the Pressure-Induced Structural Phase Transition in CeNi

Structure of CeNi high pressure-phase: Pnma symmetry

DFT calculations (VASP)

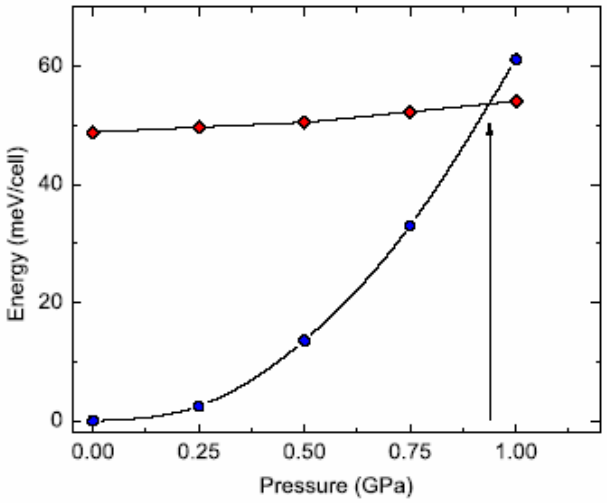

The relative energies as function of pressure for LP *Cmcm* (circles) and HP *Pnma* (diamonds) structure as obtained from DFT calculations. Arrow indicates the structural transition at pressure *P* =0.94 GPa.

DFT (LDA) calculations confirm the stability of the C*mcm* CeNi crystal structure at ambient pressure down to the lowest temperature.

At the pressure value above 1 GPa the P*nma* structure becomes preferable.

Interatomic distances (with respect to a central Ce ion):

Cmcm:

1st coordination sphere – 7 Ni neighbors

$2 \times R_1$= 2.938 Å, $4 \times R_2$= 2.948 Å, $1 \times R_3$=3.011 Å.

2nd coordination sphere – 8 Ce neighbors

$2 \times R_4$=3.601 Å, $4 \times R_5$=3.752 Å, $2 \times$R6(LP) = 3.771 Å

P*nma:*

1st coordination sphere – 6 Ni nieghbors

$1 \times R_1$=2.357 Å, $1 \times R_2$=2.761 Å, $2 \times R_3$=2.794 Å, $2 \times R_4$=2.980.

2nd coordination sphere – 8 Ce neighbors

$2 \times R_5$=3.525 Å, $2 \times R_6$=3.611 Å, $4 \times R_7$=3.773 Å.

R-Ni distances ↓ ⇒ 4f-Ni3d hybridization is expected to increase

Dynamic Magnetic Response Across the Pressure-Induced Structural Phase Transition in CeNi

Magnetic excitation spectrum of CeNi

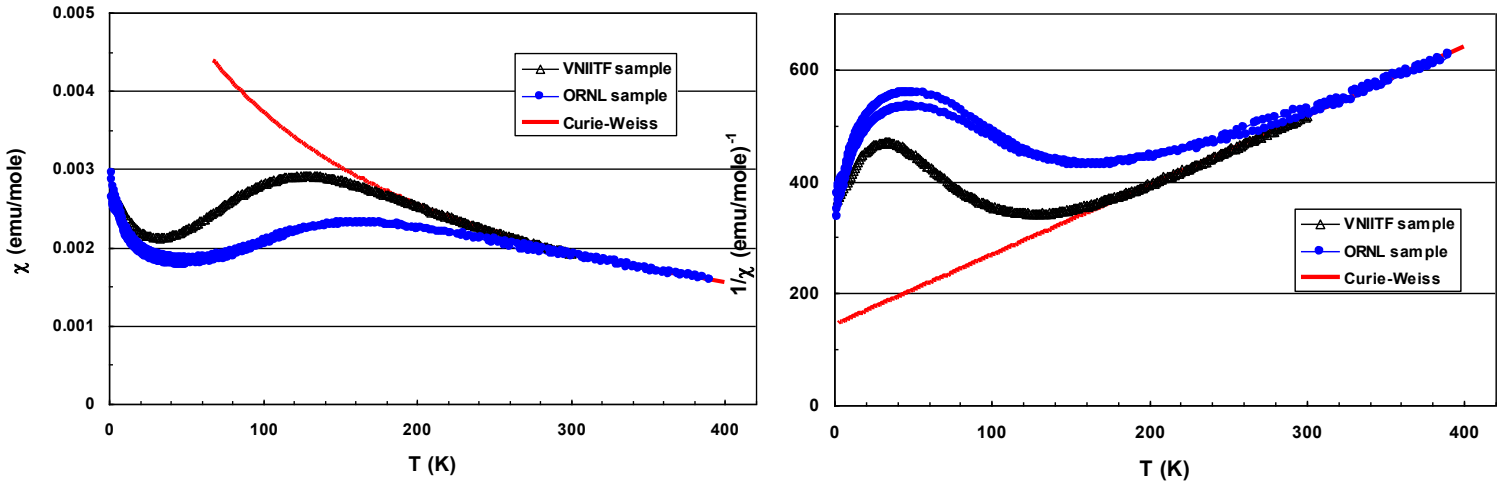

The magnetic susceptibility vs. temperature (left) and inverse magnetic susceptibility vs. temperature (right) for two powder samples of CeNi.

Red curves correspond to the Curie-Weiss law with the effective magnetic moment of free Ce^{3+} ion p = $g[(J(J+1)]^{1/2}$ = 2.53 (J=5/2). ORNL sample aws prepared for the INS experiments using ^{60}Ni isotope. VNIITF sample was prepared for previously published magnetic measurements

A. Mirmelstein et al., JNM 385, 57 (2009)]

Anomalous upturn of $\chi(T)$ below 20 K has, most probably, an intrinsic origin connected presumably with coherent f-d hybridization [V.R. Fanelli et al., J. Phys.: Condens. Matter 26, 225602 (2014); J. Aarts et al., Solid State Commun. 56, 523 (1985)]

Dynamic Magnetic Response Across the Pressure-Induced Structural Phase Transition in CeNi

Magnetic excitation spectrum of CeNi

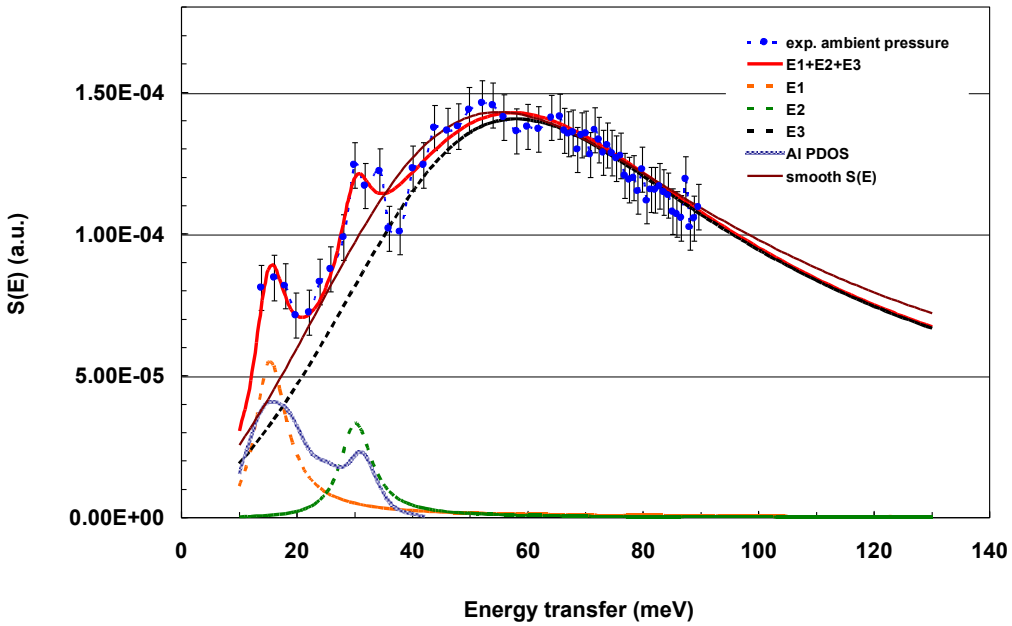

Magnetic scattering function $S_{mag}(E)$ for the polycrystalline $CeNi^{60}$ sample at T = 20 K and ambient pressure (no pressure cell).

$$S_{mag}(Q,E,T) \sim |F(Q)|^2 \frac{E}{1-\exp(-E/k_BT)} \frac{\Gamma/2}{(\Gamma/2)^2+(E-E_0)^2}$$

Γ is the full width at half maximum (FWHM) of Lorentzian spectral component. E_0 determines the characteristic energy scale of the IV system (Kondo temperature $T_K = E_0/k_B$)

E_1=15±0.2 meV, Γ/2=3.3±0.2 meV
E_2=30±0.3 meV, Γ/2=3.3±0.2 meV
E_3=40±2 meV, Γ/2=42±3 meV

Dynamic Magnetic Response Across the Pressure-Induced Structural Phase Transition in CeNi

Magnetic excitation spectrum of CeNi

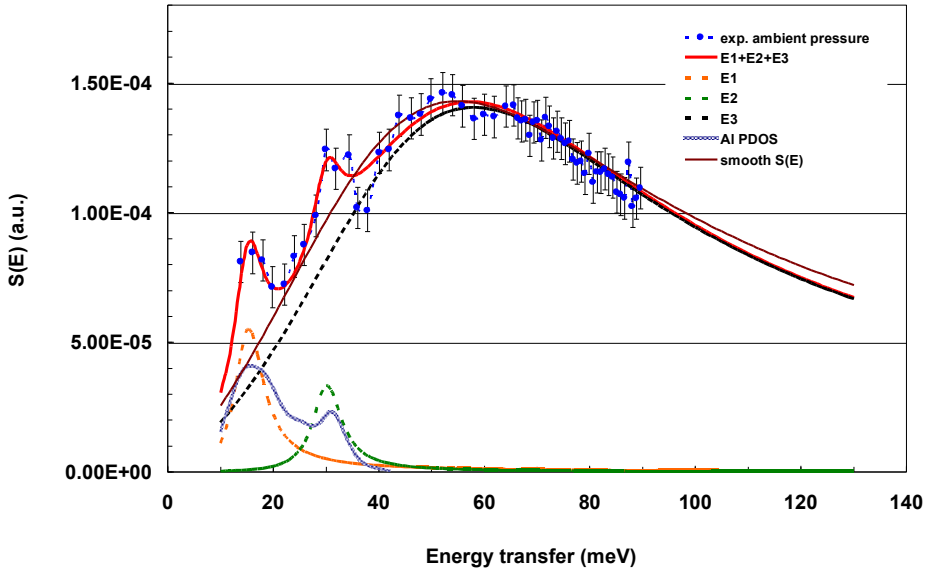

Magnetic scattering function $S_{mag}(E)$ for the polycrystalline $CeNi^{60}$ sample at T = 20 K and ambient pressure (no pressure cell).

E_1=15±0.2 meV, Γ/2=3.3±0.2 meV
E_2=30±0.3 meV, Γ/2=3.3±0.2 meV
E_3=40±2 meV, Γ/2=42±3 meV

$CeNi^{60}$ single crystal
E. Clementyev et al. PRB 61, 6189 (2000)

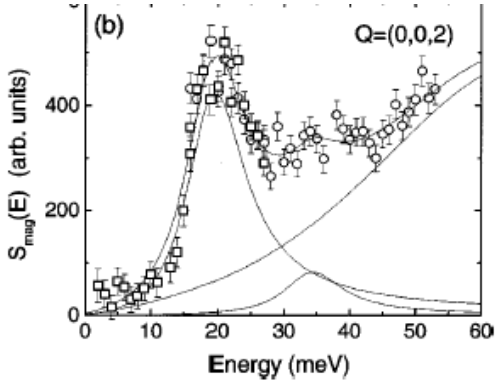

E_1~18 meV, Γ/2=4,5±0,5 meV
E_2~34 meV, Γ/2=4,5±0,5 meV
E_3~46 meV, /2 ~24 meV

E_1 and E_2 coincide with the Al PDOS maxima

The origin of two narrow spectral lines remains unknown

Dynamic Magnetic Response Across the Pressure-Induced Structural Phase Transition in CeNi

Magnetic excitation spectrum of CeNi

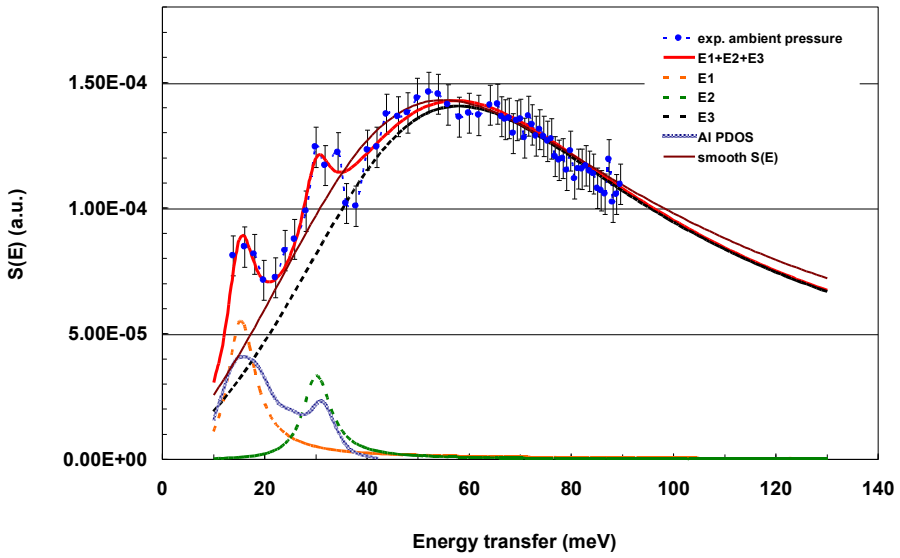

Polycrystalline $CeNi^{60}$, T=12 K, HET (ISIS, RAL)
E_i=150 meV
V.N. Lazukov et al. Europhys. Lett. 33, 141 (1996)

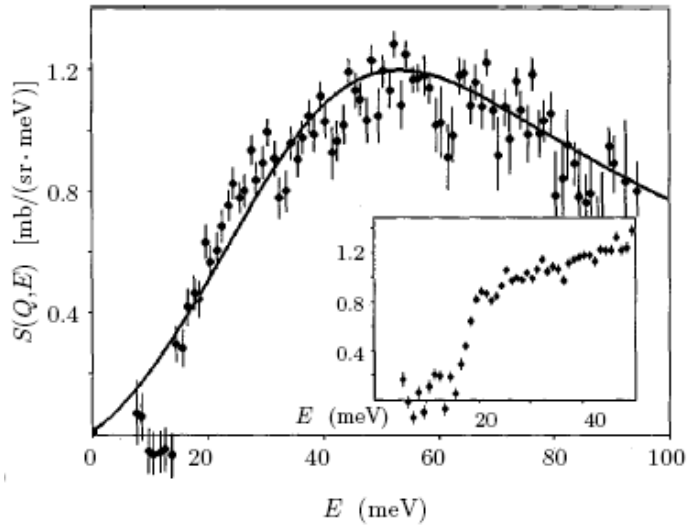

Magnetic scattering function $S_{mag}(E)$ for the polycrystalline $CeNi^{60}$ sample at T = 20 K and ambient pressure (no pressure cell).

«smooth» (brown) line:

E_0 = 33±2 meV, Γ/2 = 44±3 meV

E_0 = 33±3 meV, Γ/2 = 45±5 meV

Dynamic Magnetic Response Across the Pressure-Induced Structural Phase Transition in CeNi

Magnetic excitation spectrum of CeNi

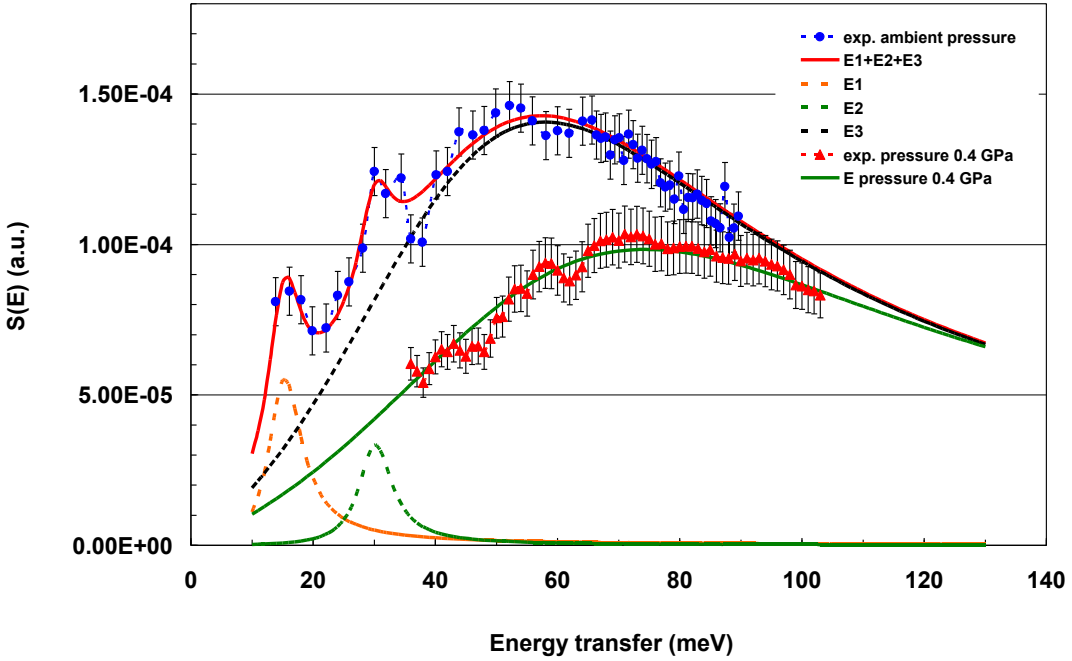

Magnetic scattering function of CeNi[60] at *T* = 20 K and ambient pressure (blue circles) and pressure of 0.4 GPa (red triangles), i.e. before and after the structural *Cmcm*→*Pnma* phase transition.

T = 20 K, ambient pressure
E_0 = 33±2 meV, Γ/2 = 44±3 meV (smooth line)

T = 20 K, P = 0.4 GPa
E_0 = 50±2 meV, Γ/2 = 55±3 meV

Compression of CeNi leads to the increase of T_K due to enhanced Ce4f-Ni3d hybridization

Dynamic Magnetic Response Across the Pressure-Induced Structural Phase Transition in CeNi

Comparison with bulk measurements [γ, Pauli-like low-temperature $\chi_0 \sim \langle n_f \rangle / E_0$)]

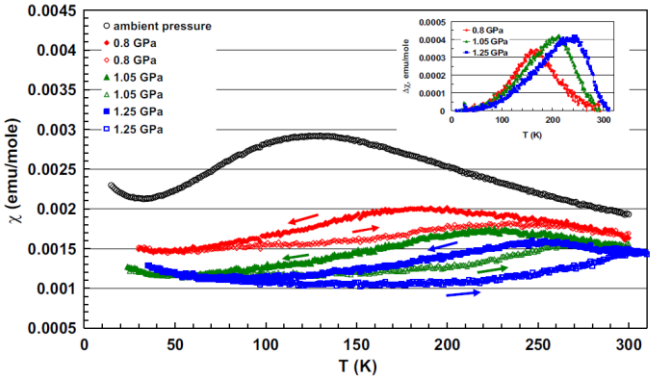

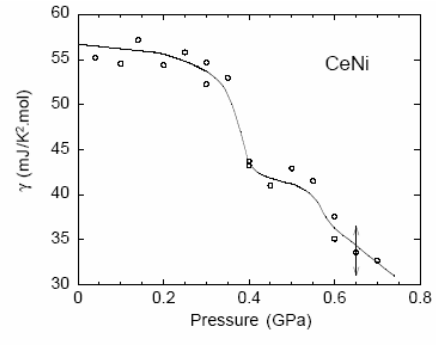

CeNi magnetic measurements
A. Mirmelstein et al., JNM 385, 57 (2009)
χ_0(T= 30 K, P=0)/χ_0(T= 30 K, P = 0.47 GPa) ≈ 1.33

CeNi specific heat
S. Takaynagi et al., J. Phys. Soc. Jap. 70 (2001) 753
γ(P=0)/γ(P=0.45GPa) ≈ 1.36, γ(P=0)/γ(P=0.6GPa) ≈ 1.63

INS experiments

E_0(P=0.4GPa)/E_0(P=0) = 50/33 = 1.52

$$\langle n_f \rangle \approx 1 - 0.05(\mathrm{meV}^{-1}) \times E_0$$

E.S. Clementyev and A.Mirmelstein JETP 109, 128 (2009)

$\langle n_f \rangle$ ≈ 0.84 (P = 0), $\langle n_f \rangle$ ≈0.75 (P = 0.4 GPa)
[$\langle n_f \rangle / E_0$($P$=0)]/[$\langle n_f \rangle / E_0$(P=0.4GPa)] = 1.69

If E_0(P=0) = 40 meV (broad E_3 line)

$\langle n_f \rangle$ ≈ 0.8(P = 0), $\langle n_f \rangle$ ≈0.75 (P = 0.4 GPa)
[$\langle n_f \rangle / E_0$($P$=0)]/[$\langle n_f \rangle / E_0$(P=0.4ГПа)] = 1.33

Consistent results of bulk and INS measurements

Dynamic Magnetic Response Across the Pressure-Induced Structural Phase Transition in CeNi

Inelastic magnetic form factor of CeNi

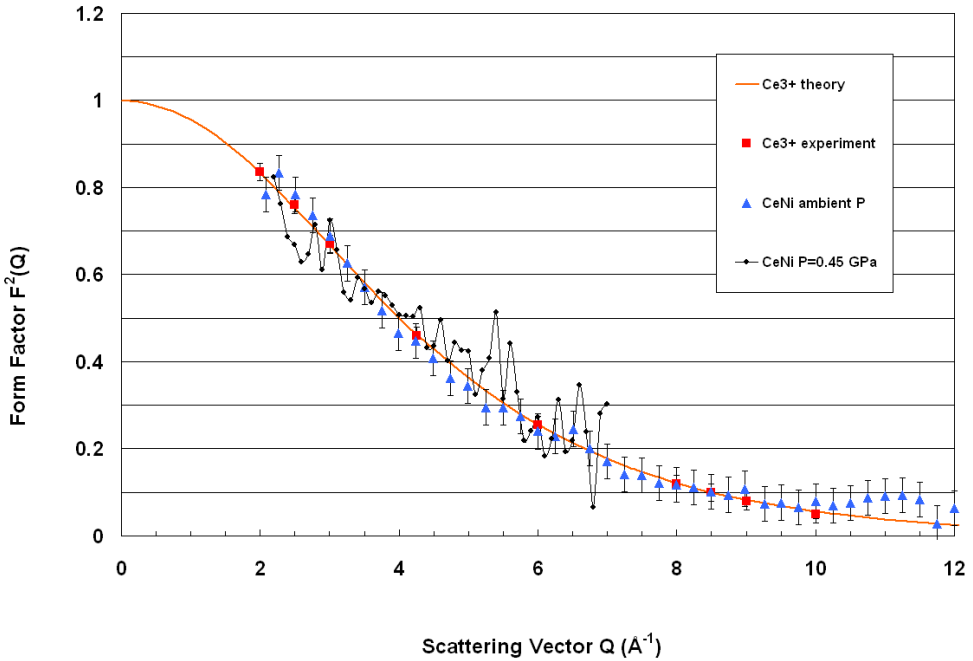

Within the energy transfer range 55 < E < 85 meV nuclear contributions becomes negligible.

Measured signal = magnetic contribution + almost Q-independent weak background.

60 < E < 80 integration window to obtain $F^2(Q)$

Magnetic form factor $F^2(Q)$ of CeNi before (blue triangles) and after (black circles) pressure-induced volume-collapse structural phase transition. The calculated form factor for the free Ce^{3+} and form factor measured experimentally for α-phase of metallic cerium [A.P. Murani, S.J. Levett, and J.W. Taylor, Phys. Rev. Lett. 95, 256403 (2005)] are shown for comparison.

Dynamic magnetic response of CeNi follows the free ion Ce^{3+} magnetic form factor before and after the structural transition in spite of essential variation of Kondo temperature and spectral response broadening.

Conclusions

- **The pressure-induced crystal structure is shown to belong to the P*nma* space group. An approximate phase diagram is suggested.**
- **The experimental results clearly demonstrate the increase of the characteristic energy scale of magnetic fluctuations (Kondo temperature) and the decrease of effective occupation of the $4f^1$ (J=5/2) ground state of the collapsed phase due to the enhanced Ce4f-Ni3d hybridization.**
- **The space distribution of magnetic density does not change under transition and remains the same as in the free Ce^{3+} ion.**

4f electrons remains localized, while strongly hybridized with conducting bands, in the CeNi P*nma* structure

as well as in the case of $\gamma \rightarrow \alpha$ transition in cerium.

*C.-K. Loong et al. Phys. Rev. B **35** 3092 (1987)*
*A.P. Murani, S.J. Levett, and J.W. Taylor, Phys. Rev. Lett. **95**, 256403 (2005)*
*B. Chakrabarti, M.E. Pezzoli, G. Sordi, K. Haule, G. Kotliar, Phys. Rev. B **89**, 125113 (2014)*

Is E_0 (T_K) the only direct measure of localization/delocalization degree which can be determined experimentally?

Theory of $\gamma \rightarrow \alpha$ transition in Ce

DFT+DMFT calculations of F(Q) and Imχ(Q,E) $\Rightarrow$ KVC mechanism of $\gamma \rightarrow \alpha$ transition in Ce metal:
B. Chakrabarti, M.E. Pezzoli, G. Sordi, K. Haule, G. Kotliar, PRB **89** (2014) 125113
a charge self-consistent implementation, GGA functional in WIEN2K package, continuous-time quantum Monte Carlo impurity solver. T = 116 K, Hubbard potential U=6 eV, intra-atomic exchange (Hund's coupling) J=0.7 eV.

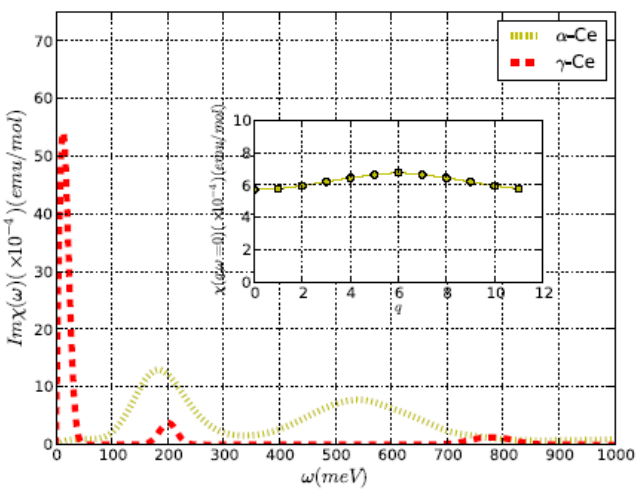

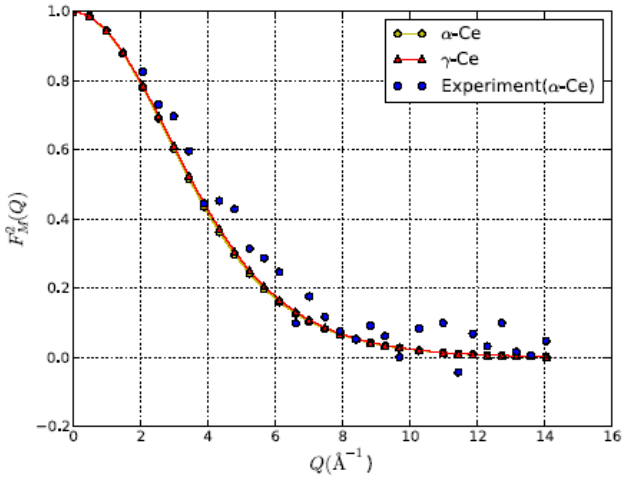

Imaginary part of the local dynamic susceptibility Im$\chi(\omega)$ for γ- and α-Ce (left). Inset: q-dependence of local static susceptibility $\chi(q, \omega = 0)$ of α-Ce.

Dispersionless character of $\chi(q, \omega = 0)$ proves the use of single-ion approach to calculate F(Q) and is consistent with the fact that magnetic form factor does not change due to transition and keeps the form of a free Ce3+ ion (right).

γ-phase: T_K ~ 10 meV, α-phase: T_K ~ 180 мэВ

Volume changes occurs due to increase in T_K and enhanced f-spd hybridization

Theory of $\gamma \rightarrow \alpha$ transition in Ce

Hybridization, T_K, and spin-orbit coupling in Ce

N. Lanata, Yong-Xin Yao, Cai-Zhuang Wang, Kai-Ming Ho, Jörg Schmalian, Kristjan Haule, and Gabriel Kotliar, PRL **111**, 196801 (2013). LDA+GA, analog of LDA+DMFT (slave bosons to solve an impurity problem)

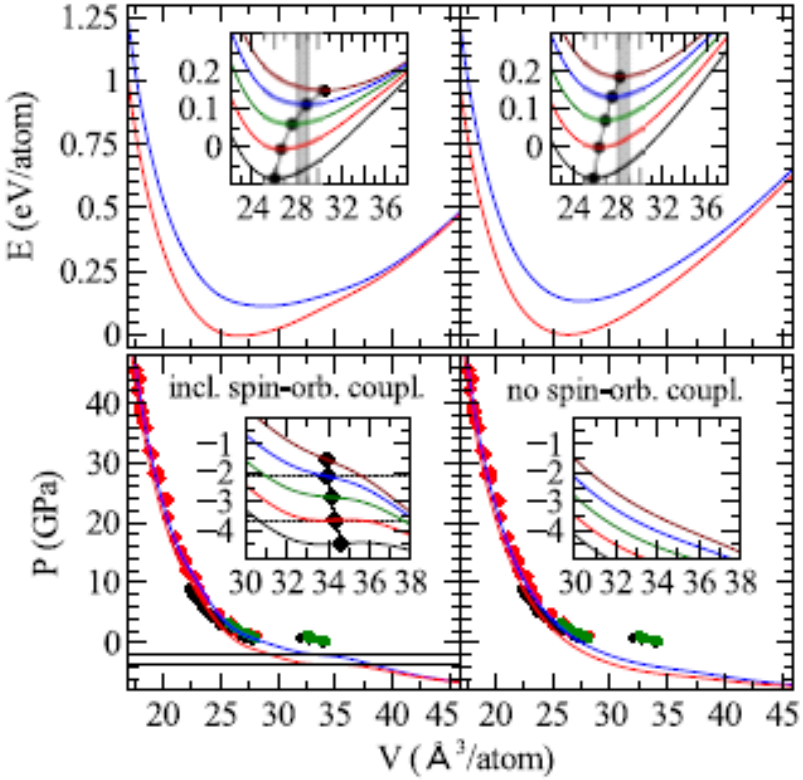

Total energy vs. volume (top) and P-V curves (bottom) for U=5 eV and *J*=0.7 eV at T=0. и эксперимент при T=300 K (внизу). Inset: the same curves for 4.5 ≤ U ≤ 6.5 eV (step 0.5 eV) from the bottom to the top. Color signs – experimental data at 300 K. Horizontal lines (left bottom panel) and black signs in the inset indicate pressure corresponding to the minimum of bulk modulus *K*=-VdP/dV.

Pressure is calculated as P = -dE/dV. Structural transition corresponds to the minimum of *K*. At U ≤ 5.5 eV *K* changes sign, indicating the first order transition. At U = 5.5 эВ *K*=0, i.e. the second order transition.

Such a behavior is observed only in the case if spin-orbit coupling is taken into account.

Theory of $\gamma \rightarrow \alpha$ transition in Ce

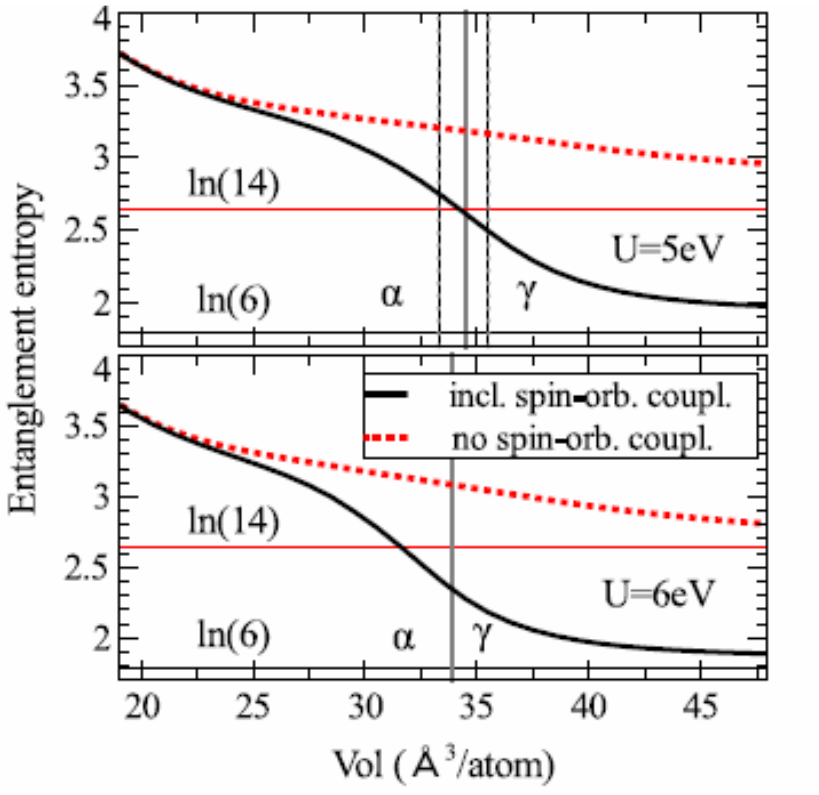

Dependence of S_f on Ce atomic volume for U = 5 eV (top) and U = 6 eV (bottom) at fixed value of *J* = 0.7 eV with (lines) and without (points) spin-orbit interaction. 14 is the dimension of single-particle local f electron space, and 6 = 2×5/2 + 1 is the degeneracy of the 5/2 eigenspace f at $n_f = 1$.

Local entanglement entropy S_f of the f electrons serves as a measure of coupling between f electrons and the rest of the environment:

$$S_f[\rho_f] = -\mathrm{Tr}[\rho_f \ln \rho_f]$$

ρ_f – reduced density matrix of the system in the f local subspace..

Crossover occurs only if SO coupling is taken into account.

In the α-phase S_f is not sensitive to the spin-orbit splitting. The local fluctuations induced in the f local space by the coupling with its environment are very large.
By increasing the volume, the fluctuations between J=5/2 f^1 subspace and the other local configurations are increasingly suppressed.
The crossover points identifies the situation in which the fluctuations are sufficiently small to be hampered by the spin-orbit.

The fluctuations are generated only by the entanglement, the main source of which is the f-spd hybridization.

Theory of $\gamma \rightarrow \alpha$ transition in Ce

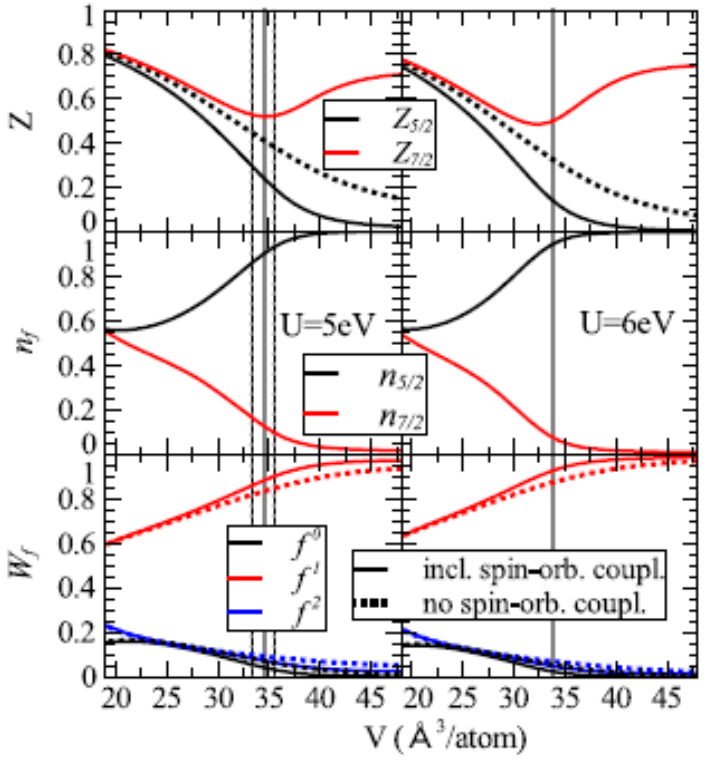

Quasiparticle renormalization weights of the 7/2 and 5/2 f electrons, 7/2 and 5/2 orbital populations, and f configuration probabilities as a function of the system volume.

1. Different behavior of Z with and without spin-orbit coupling.
2. Different behavior of Z for 5/2 and 7/2 states at the crossover point.
5/2 electrons undergo a clear crossover towards a localized phase ”disentangled” by the conduction electrons.
7/2 electrons remain screened, but rapidly disappear and are absent in the γ phase.
3. Spin-orbit coupling speeds up the formation of the $4f^1$ local moment ($4f^1$ grows faster with SOC than without).

Un the α-phase, at small V, the f levels are strongly hybridized with the conduction electrons, and Z are only weakly depend on the SOC. In this regime, the system effectively behaves as if the f-level degeneracy was of the order of magnitude of 14. In the γ phase, at large V, the SOC becomes more important and substantially reduces the effective f-level degeneracy.

Thank you very much for your attention!

Dynamic Magnetic Response Across the Pressure-Induced Structural Phase Transition in CeNi

Magnetic excitation spectrum of CeNi

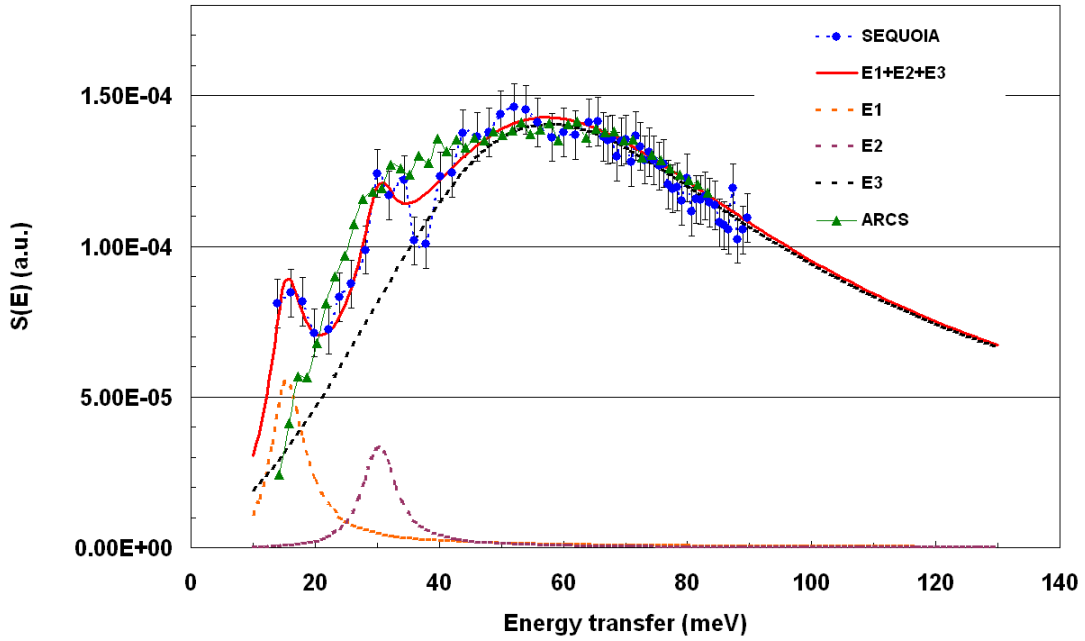

Magnetic scattering function of $CeNi^{60}$ at ambient pressure (no cell) measured at T = 20 K with spectrometer SEQUOIA (blue circles) and at T = 12 K with ARCS instrument.

Theory of $\gamma \rightarrow \alpha$ transition in Ce

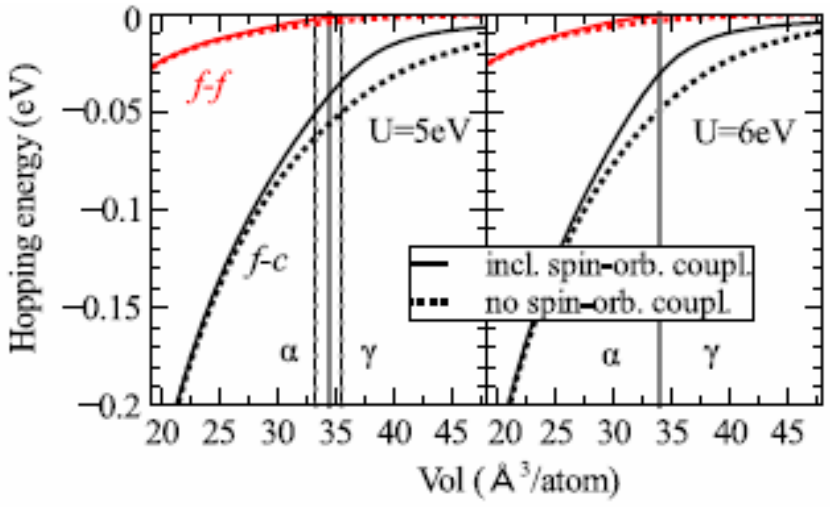

Ожидаемые для основного состояния величины энергий **f-c** (Кондо) и **f-f** (Хаббард) перескоков в зависимости от атомного объема системы для двух значений U = 5 эВ (слева) и 6 эВ (справа). Вертикальные линии – границы переходов

Ожидаемые для основного состояния величины энергетических компонент эффективного Гамильтониана , основное состояние которого обеспечивает решение рассматриваемой задачи. Нелокальная часть $\hat{H}$ может быть представлена в виде

$$\hat{T} = \hat{T}_{ff} + \hat{T}_{fc} + \hat{T}_{cc}$$

где c = spd, а три члена суммы - нелокальные перескоки между f-f, f-c и c-c электронами.

Энергии перескоков f-f и f-c представляют собой масштаб энергий Хабарда и Кондо. Масштаб Кондо почти на порядок превышает масштаб Хаббарда, который $\rightarrow$ 0 вблизи перехода. Это соответствует KVK модели изоструктурного перехода. Можно заключить, что основной источник связывания f локального пространства и его окружения – f-spd гибридизация. При учете СО взаимодействия энергетический масштаб Кондо уменьшается быстрее вблизи перехода, чем без учета СОВ.

Фазовые переходы с коллапсом объема в f-электронных системах: Ce, теория

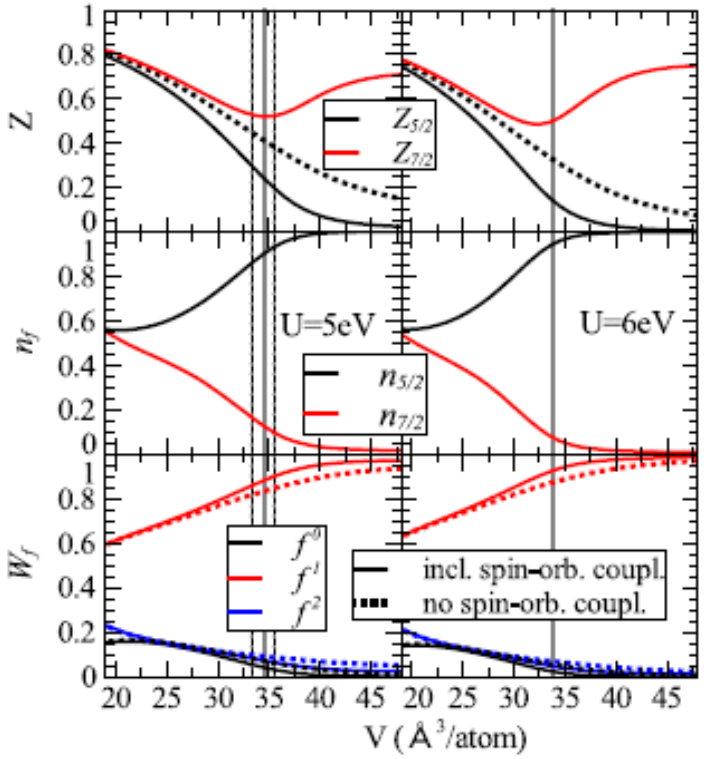

Факторы перенормировки Z квазичастичного спектра для 7/2 и 5/2 f электронов (верхняя панель), орбитальные заселенности (в середине) и вероятности f конфигураций как функции атомного объема церия. Приведены значения этих параметров при U = 5 эВ (слева) и U = 6 эВ (справа) с учетом и без учета СО взаимодействия.

Даже в γ-фазе, до коллапса, в основном состоянии есть примесь f^2 конфигурации, причем, судя по рисунку, ее даже больше, чем f^0.

Перераспределение между 5/2 и 7/2 состояниями – более резкий эффект вблизи перехода, чем изменение вероятностей конфигураций

При уменьшении вероятности конфигурации f^1 растет вероятность конфигурации f^2, так что $N_f \sim 1$, а при малом объеме $N_f > 1$.

Вероятность f^0 в области перехода растет незначительно.

Все вероятности, независимо от учета СОВ, изменяются практически монотонно в области перехода. тронов.

При $U=U_c \sim 5.5$ эВ – квантовая критическая точка II рода фазовой диаграммы Следовательно, металлический церий – критический элемент (J.C. Lashley et al, PRL **97** (2006) 235701)

Влияние температуры на физику α-γ превращения: N. Lanata, Yong-Xin Yao et al., PRB **90**, 161104(R) (2014)

Структура фазы высокого давления CeNi

Оставалась неизвестной с 1985 г.

Структура CeNi
при нормальном давлении

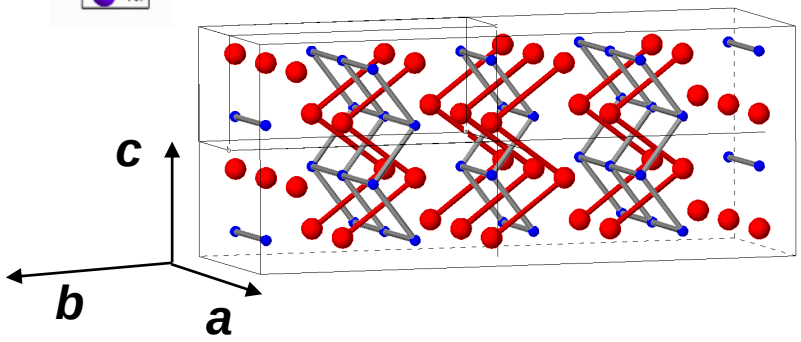

Основной структурный мотив: чередующиеся треугольники (тригональные призма), построенные из Ce либо Ni

Орторомбическая структура типа CrB

Пространственная группа *Cmcm*

a = 3.77 Å, *b* = 10.543 Å, *c* = 4.37 Å

Ce: 4c (0, 0.14, 1/4)

Ni: 4c (0, 0.42, 1/4)

T = 300 K

Структура фазы высокого давления, *T*=298 K, *P*=4.2

Орторомбическая структура типа FeB (пр. гр. P*nma*)

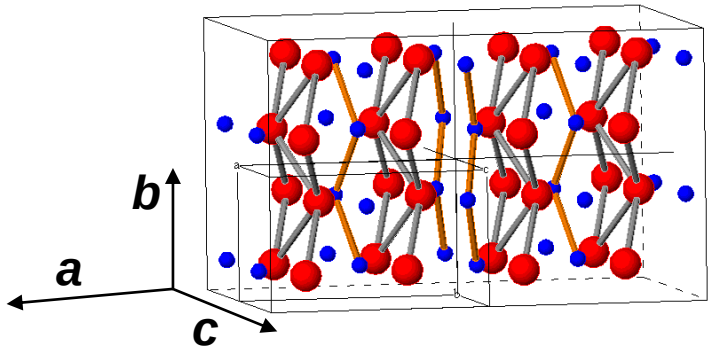

Если в P*nma* (0.403, 0.25, 0.101) z = 0 ⇒ C*mcm*

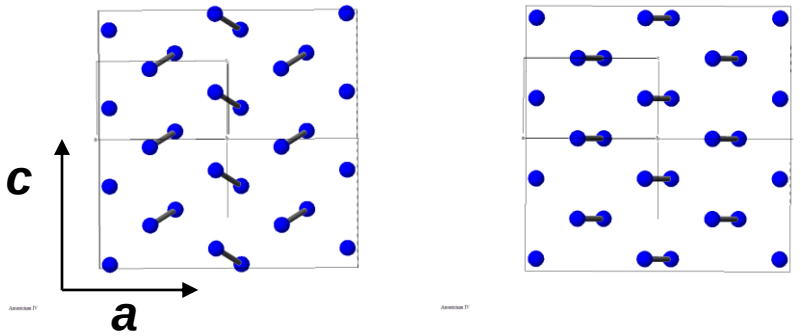

CrB структура типична для RNi, где R – из первой половины P3 серии, а FeB – для R из второй половины P3 серии

What is intermediate valence (IV)?

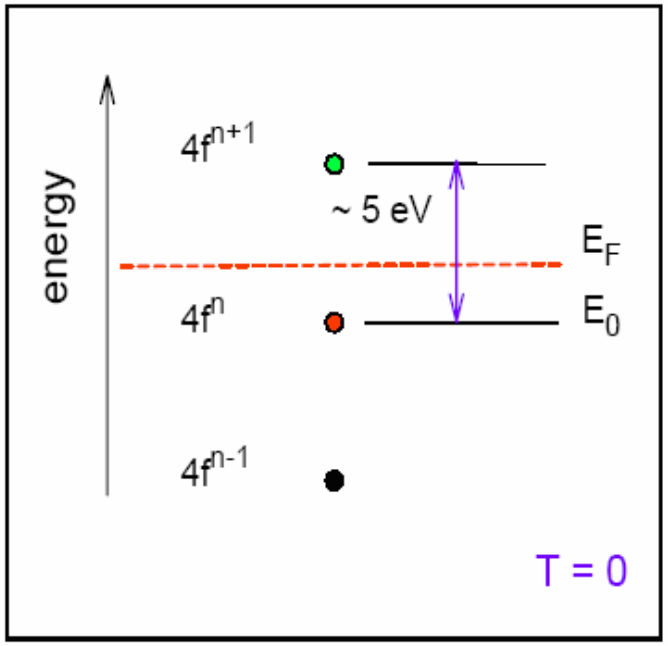

Energy of 4*f* level of isolated impurity at T = 0

E_0– energy of unperturbed $4f^n$ level
Coulomb repulsion ~ 5 eV
***s*- and *p*- conducting electrons + localized *f* electrons**

Charge and spin transfer (fluctuations) between *f- and* (*s,p*) electrons

+ hybridization $\Gamma = \pi^2 V^2 N(E_F)$

$\Gamma << E_0$ – stable 4f shell

$\Gamma < E_0$ – heavy fermions

$\Gamma \geq E_0$ – intermediate (non-integer) valence (3.2+)